CHANNEL IMPULSIVE NOISE MITIGATION FOR LINEAR VIDEO CODING SCHEMES

S. Zheng, M. Cagnazzo

LTCI, Télécom ParisTech,
Univ Paris-Saclay, 75013 Paris, France.

M. Kieffer

L2S, CNRS–CentraleSupelec–Univ Paris-Sud,
Univ Paris-Saclay, 3 rue Joliot-Curie,
91192 Gif-sur-Yvette, France.

ABSTRACT

This paper considers the problem of impulse noise mitigation for videos encoded using a SoftCast-based Linear Video Coding (LVC) scheme and transmitted using an OFDM scheme over a wideband channel prone to impulse noise. In the time domain, the impulse noise is modeled as realizations of iid Bernoulli-Gaussian variables. A Fast Bayesian Matching Pursuit algorithm is employed for impulse noise mitigation. This approach requires the provisioning of some OFDM subchannels to estimate the impulse noise locations and amplitudes. Provisioned subchannels cannot be used to transmit data and lead to a decrease of the nominal decoded video quality at receivers in absence of impulse noise. Using a phenomenological model (PM) of the residual noise variance after impulse correction, an algorithm is proposed to evaluate the optimal number of subchannels to provision for impulse noise mitigation. Simulation results show that the PM can accurately predict the number of subchannels to provision and that impulse noise mitigation can significantly improve the decoded video quality compared to a situation where all subchannels are used for data transmission.

***Index Terms*—** Video transmission, SoftCast, OFDM, Impulse noise mitigation, Joint source-channel coding.

1. INTRODUCTION AND MAIN CONTRIBUTIONS

SoftCast [9] based Linear video coding (LVC) and transmission schemes [2, 4–8, 10, 13–15, 19, 23–28] have emerged as a promising alternative to classical video coding [20–22] when video has to be transmitted to wireless receivers experiencing different and time-varying channel conditions. In LVC, the video content is encoded with linear-only operators, such as a full-frame Discrete Cosine Transform (DCT) and using linear channel precoding of these DCT coefficients. Since the transmitted symbols are linearly related to the original video pixel values and a Linear Minimum Mean Square Error (LMMSE) estimator is used at receiver side, the decoded video quality scales linearly with the channel signal-noise-ratio (SNR) [9].

In this paper, we address the problem of impulse noise mitigation when the LVC-encoded video is transmitted using an Orthogonal Frequency-Division Multiplexing (OFDM) scheme over a wideband channel prone to impulse noise. Several types of communication channels may be also prone to impulse noise, *e.g.,* Digital Subscriber Line (DSL) [16], or in Power Line Telecommunications (PLT) channels [30]. Impulse noise has a high amplitude (its power may be 50 dB above that of the background noise), and when it is bursty, may corrupt the channel for more than 1 ms. If impulse noise is not corrected, the communication performance may be significantly degraded [1, 12]. As in [1], the impulse noise is modeled in the time domain as realizations of independent and identically distributed (iid) Bernoulli-Gaussian variables. In our paper a Fast Bayesian Matching Pursuit (FBMP) [18] algorithm is employed for impulse noise mitigation. This approach requires the provisioning of some OFDM subchannels to estimate the impulse noise locations and amplitudes. Since nothing can be transmitted on provisioned subchannels, this leads to a decrease of the number of transmitted LVC samples and to a decrease of the nominal video quality at receivers in absence of impulse noise. A trade-off has thus to be found between impulse noise correction efficiency and nominal PSNR reduction.

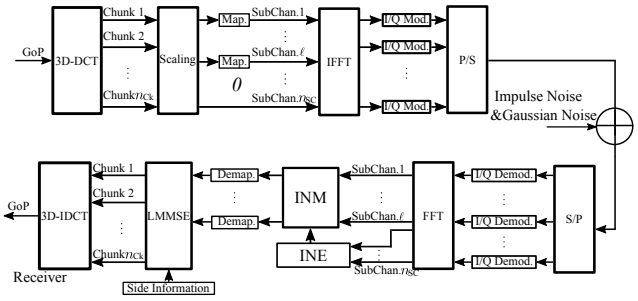

Fig. 1: Proposed transmitter and receiver architectures for modified SoftCast-based LVC with subchannel provisioning and impulse noise mitigation.

Compared to the state-of-the-art, our contributions are (*i*) an adaptation of the FBMP algorithm to LVC schemes for channel impulse noise mitigation, see Section 2; (*ii*) the proposition of a phenomenological model (PM) structure to describe the variance of the residual noise after impulse noise correction, Section 3; (*iii*) an optimization approach to determine the optimal number of subchannels to provision for impulse noise mitigation. Simulation results in Section 4 illustrate the performance improvements provided by the proposed impulse noise mitigation scheme.

2. IMPULSE NOISE MITIGATION SCHEME FOR LVC

In this section we present the architecture of the proposed impulse noise mitigation scheme for SoftCast-based [9] LVC shown in Fig. 1. In this paper we focus on Scaling, Impulse Noise Estimation (*INE*), Impulse Noise Mitigation (*INM*), and decoding (LMMSE) modules, while the other steps are the same as in [9].

The input video is organized in Group of Pictures (GoP); each GoP undergoes 3D-DCT and the resulting coefficients are organized in blocks called chunks of dimension $n_{\mathrm{r}} \times n_{\mathrm{c}}$. The number of chunks

per GoP is n_{Ck}. The chunks are scaled and used to modulate the carriers of an OFDM-based transmission scheme with n_{SC} subchannels; a total power p_{T} is available for each OFDM symbol. In this paper, we focus on the luminance part of the video. The chrominance components undergo a similar processing.

To perform scaling and transmission, $n_{\text{r}} \times n_{\text{c}}$ *chunk vectors* t_i, $i = 1, \ldots, n_{\text{r}} \times n_{\text{c}}$, each of dimension n_{Ck}, are formed by selecting for each vector one coefficient per chunk. The t_is can be seen as realizations of $n_{\text{r}} \times n_{\text{c}}$ iid Gaussian vectors with covariance matrix $\Lambda = \text{diag}(\lambda_1 \ldots \lambda_{n_{\text{Ck}}})$. Without loss of generality, the chunks, are assumed to be sorted according to decreasing variance λ_j, $j = 1, \ldots, n_{\text{Ck}}$. The chunk vectors are multiplied (scaled) by a diagonal precoding matrix $G \in \mathbb{R}^{n_{\text{SC}} \times n_{\text{Ck}}}$ [9, 11, 29] designed in such a way that $u_i = Gt_i$ satisfies a power constraint $p_{\text{T}}/2$. We focus on a bandwidth constrained scenario where $n_{\text{SC}} \leqslant n_{\text{Ck}}$. In this case, only the n_{SC} chunks of largest variance can be transmitted [9]. Moreover, due to the total power constraint, it is possible that the q lowest-variance chunks must further be discarded [11, 29]. In the proposed architecture, it is possible to discard chunk even when there is enough available transmission power, since this operation will improve the robustness to impulse noise, as shown later on. In any case, when we discard q chunks, the last q rows of G are null.

Then, $n_{\text{r}} \times n_{\text{c}}/2$ vectors of complex symbols are formed by combining pairs of consecutive scaled chunk vectors: $\widetilde{u}_i = G\left(t_{2i-1} + jt_{2i}\right)$, $i = 1, \ldots, n_{\text{r}} \times n_{\text{c}}/2$, the power of $\widetilde{u}_i$ is p_{T}. Next the $\widetilde{u}_i$s are used to modulate the OFDM carriers in a standard way. For the sake of simplicity, in what follows the index i is omitted, since all vectors $\widetilde{u}_i$ have similar distribution and undergo the same processing. In the plain Softcast, a Hadamard transform is performed after chunk scaling. Here, to simplify presentation, this additional transform is not considered.

The transmitted signal is assumed to be corrupted by Gaussian noise and impulsive noise. At the receiver side, the input of the FFT is a vector $y \in \mathbb{C}^{n_{\text{SC}}}$ that may be modeled as in [1]

$$y \quad = \quad F^H \widetilde{u} + v_{\text{I}} + v_{\text{g}}, \tag{1}$$

where F^H is IDFT matrix, v_{g} is a Gaussian noise vector and v_{I} is an impulse noise vector. After the DFT, $Fv_{\text{g}} \sim \mathcal{CN}\left(0, N_{\text{g}}\right)$ can be modeled as a zero-mean complex circular Gaussian noise vector [1] with $N_{\text{g}} = 2N$ and $N = \text{diag}\left(\sigma_1^2, \ldots, \sigma_{n_{\text{SC}}}^2\right)$, without loss of generality, one assumes that the subchannel indexing is such that $\sigma_1^2 \leqslant \cdots \leqslant \sigma_{n_{\text{SC}}}^2$. The components of v_{I} are iid and such that $v_{\text{I},k} = \delta_k w_k$, where δ_k is the realization of a Bernoulli variable with parameter $p_{\text{I}} = \Pr\{\delta_k = 1\}$ and $w_k \sim \mathcal{CN}\left(0, 2\sigma_{\text{I}}^2\right)$ with $\sigma_{\text{I}}^2 > \sigma_j^2$, $j = 1, \ldots, n_{\text{SC}}$.

Since the q last rows of G are null, we can introduce the *parity-check matrix* $\Psi \in \mathbb{C}^{q \times n_{\text{SC}}}$ formed by the q last rows of F, and $\Psi F^H G = 0$. Then one may evaluate the *syndrome vector*

$$\begin{aligned} s &= \Psi y \\ &= \Psi v_{\text{I}} + \Psi v_{\text{g}}, \end{aligned} \tag{2}$$

where $\Psi v_{\text{g}} \sim \mathcal{CN}\left(0, N_s\right)$, with $N_s = 2\text{diag}\left(\sigma_{n_{\text{SC}}-q+1}^2, \ldots, \sigma_{n_{\text{SC}}}^2\right)$. Therefore to mitigate the effect of the impulse noise, one has to estimate the sparse vector v_{I} from noisy measurements of Ψv_{I}. This is a typical compressive sensing estimation problem [3] for which many solutions have been proposed. Here, the FBMP algorithm [18] is employed to get an estimate $\widehat{v}_{\text{I}} = \text{E}\left(v_{\text{I}}|s\right)$ of v_{I}. This step correspond to the *INE* block in Fig. 1. Finally, after impulse noise mitigation one evaluates

$$\begin{aligned} \widehat{y} &= Fy - F\widehat{v}_{\text{I}} \\ &= \widetilde{u} + F\left(v_{\text{I}} - \widehat{v}_{\text{I}}\right) + Fv_{\text{g}}. \end{aligned} \tag{3}$$

This step correspond to the block *INM* in Fig. 1. In what follows, this scheme is called LVC With Subchannel Provisioning and Impulse Correction (LVC-WSP-IC). The main difficulty lies in the optimization of the number q of subchannels provisioned for impulse noise mitigation. A solution to this problem is detailed in Section 3.

3. OPTIMAL NUMBER OF PROVISIONED SUB-CHANNELS

As shown in [18], the efficiency of the FBMP algorithm increases with the number q of observations of linear combinations of the impulse errors (2). Increasing q, however, reduces the number of subchannels on which chunks can be transmitted. A trade-off has thus to be found between efficiency of impulse noise correction and transmission performance.

3.1. Residual noise after impulse noise mitigation

One may rewrite (3) as

$$\widehat{y} = \widetilde{u} + Fv_{\text{r}} + Fv_{\text{g}}, \tag{4}$$

where $v_{\text{r}} = v_{\text{I}} - \widehat{v}_{\text{I}}$ represents the impulse noise residual vector after mitigation. This residual can be seen as an additional noise component to the background Gaussian noise affecting the sub-channels.

As shown in [1], the covariance matrix of the impulse noise residual $\text{Cov}\left(v_{\text{r}}|s\right)$ can be approximated as diagonal, provided that n_{SC} and q are large enough. Therefore, the covariance matrix of $Fv_{\text{r}}|s$ $\text{Cov}\left(Fv_{\text{r}}|s\right) = F\text{Cov}\left(v_{\text{r}}|s\right)F^H$ has its diagonal elements equal to $\sigma_{\text{r}}^2 = \text{Tr}\left(\text{Cov}\left(v_{\text{r}}|s\right)\right)/n_{\text{SC}}$. Clearly, the off-diagonal entries in $\text{Cov}\left(Fv_{\text{r}}|s\right)$ are not zero, but they are neglected in what follows to get

$$\text{Cov}\left(Fv_{\text{r}}|s\right) \approx \sigma_{\text{r}}^2 I. \tag{5}$$

Considering (4) and (5), the vectors Gt_{2i} and Gt_{2i+1} are corrupted respectively by the real and imaginary parts of Fv_{r} and Fv_{g}, with $Fv_{\text{r}} \sim \mathcal{CN}\left(0, \sigma_{\text{r}}^2 I\right)$. Assuming that Fv_{r} and Fv_{g} are uncorrelated, each component of Gt_{2i} and Gt_{2i+1} will be corrupted by a zero-mean Gaussian noise with variance $\sigma_{\text{c},j}^2 = \sigma_j^2 + \sigma_{\text{r}}^2/2$. By using this in the design of the optimal precoding matrix and decoding matrices, the MSE of the received chunk vector $E\left[\left\|\left(t - \widehat{t}\right)\right\|_2^2\right]$ [11, 29] is

$$\varepsilon = \sum_{j=\ell+1}^{n_{\text{Ck}}} \lambda_j + \sqrt{\gamma} \sum_{j=1}^{\ell} \sqrt{\lambda_j \sigma_{\text{c},j}^2}, \tag{6}$$

where $\ell = n_{\text{SC}} - q$ and $\sqrt{\gamma} = \frac{\sum_{j=1}^{\ell} \sqrt{\lambda_j \sigma_{\text{c},j}^2}}{\frac{p_{\text{T}}}{2} + \sum_{j=1}^{\ell} \sigma_{\text{c},j}^2}$.

3.2. Estimation of σ_{r}^2

From [18], one knows that σ_{r}^2 depends on q, N_{g}, σ_{I}^2, and p_{I}. An explicit expression of the evolution of σ_{r}^2 is very difficult to obtain. Thus, in this section, we will resort to a phenomenological model (PM) of σ_{r}^2 as a function of these parameters. First experiments have been conducted to characterize the structure of the model. Then the value of the model parameters are estimated via least-square estimation.

Two main channels with $n_{\text{SC}} = 256$ subchannels and $n_{\text{SC}} = 416$ subchannels are considered here. For both channels, Gaussian background noise with $N_{\text{g}} = 2\sigma_{\text{g}}^2 I$ and impulse noise $\sigma_{\text{I}}^2 = 100$ are introduced. The variance of the background noise is adjusted in such a way that the *impulsive to background noise ratio* (INR) in

dB, *i.e.*, $10\log_{10}\left(\sigma_{\mathrm{I}}^2/\sigma_{\mathrm{g}}^2\right)$ ranges from 10 dB to 30 dB with a step of 2 dB. The impulse probability p_{I} ranges from 0.5% to 3% with a step of 0.5%. Under these channel conditions, σ_{r}^2 is evaluated as the average of $\|v_{\mathrm{I}} - \widehat{v}_{\mathrm{I}}\|_2^2$. One evaluates σ_{r}^2 considering different proportions of unused subchannels $r_{\mathrm{d}} = \frac{q}{n_{\mathrm{SC}}}$ ranging from 0.15 to 0.75 with a step of 0.05. Since the FBMP only uses the syndrome (2), which does not depend on the transmitted chunks, all evaluations are performed assuming that all-zero chunks are transmitted.

From the experimental results, one observes that $\log_{10}\left(\sigma_{\mathrm{r}}^2\right)$ can be represented as a function of $(1-r_{\mathrm{d}})^2$, $\mathrm{INR}_{\mathrm{dB}}$ and $\log_{10}(p_{\mathrm{I}})$ and shows an almost linear dependency on each variable when the others are fixed. Therefore one may approximate $\log_{10}\left(\sigma_{\mathrm{r}}^2\right)$ as

$$\log_{10}\left(\sigma_{\mathrm{r}}^2\right) = \mu_0\left(r_{\mathrm{d}}, \mathrm{INR}_{\mathrm{dB}}\right) + \mu_1\left(r_{\mathrm{d}}, \mathrm{INR}_{\mathrm{dB}}\right)\log_{10}(p_{\mathrm{I}}), \quad (7)$$

where $\mu_i\left(r_{\mathrm{d}}, \mathrm{INR}_{\mathrm{dB}}\right)$, $i = 0, 1$ are considered to have structure as $\mu_i\left(r_{\mathrm{d}}, \mathrm{INR}_{\mathrm{dB}}\right) = \mu_{i,0} + \mu_{i,1}\mathrm{INR}_{\mathrm{dB}} + \mu_{i,2}\left(1-r_{\mathrm{d}}\right)^2 + \mu_{i,3}\left(1-r_{\mathrm{d}}\right)^2\mathrm{INR}_{\mathrm{dB}}$.

Considering all collected data, and using the PM (7), one may easily get a least-square estimate of the value of the parameter vectors $\boldsymbol{\mu}_i = (\mu_{i,0}, \ldots, \mu_{i,3})$, $i = 0, 1$. One gets $\boldsymbol{\mu}_0^{256} = (2.6,\ -0.14,\ -1.71,\ 0.29)$, $\boldsymbol{\mu}_1^{256} = (0.71,\ -0.003,\ -0.92,\ 0.1)$ for the channel with 256 subchannels, $\boldsymbol{\mu}_0^{416} = (2.6, -0.12, -1.79,\ 0.27)$, $\boldsymbol{\mu}_1^{416} = (0.72,\ 0.007,\ -0.93,\ 0.09)$ for the channel with 416 subchannels. One observes that both sets of parameters have very close values. By using estimated parameter vectors $\boldsymbol{\mu}_0$ and $\boldsymbol{\mu}_1$, in most of the cases, estimated σ_{r}^2s from model (7) are very close to the values obtained experimentally, the maximum gap is 2.6 with ratio 40% compared to experimental value. Consequently, the PM (7) provides a good estimate of σ_{r}^2 and can be used in (6) to evaluate the total distortion.

3.3. Optimization of sub-channel provisioning

This section describes the optimization of the number q of subchannels to provision for impulse noise mitigation, as a function of N_{g}, σ_{I}^2, p_{I}, p_{T}, n_{SC} and the vector of chunk variances $(\lambda_1 \ldots \lambda_{n_{\mathrm{Ck}}})$. Here, one assumes a point-to-point communication.

For a given value of $r_{\mathrm{d}} = \frac{q}{n_{\mathrm{SC}}}$,

1. Evaluate σ_{r}^2 from the PM (7),
2. Get the target number of transmitted chunks as $\ell_{\mathrm{t}} = n_{\mathrm{SC}} - q$,
3. Obtain the chunk reconstruction MSE $\varepsilon\left(r_{\mathrm{d}}\right)$ from (6).

At Step 3, the actual number ℓ of transmitted chunk may be less than the target number ℓ_{t} due to power constraint [11, 29].

Any tool to minimize $\varepsilon\left(r_{\mathrm{d}}\right)$ may then be used, *e.g.* gradient descent, to find

$$\widehat{r}_{\mathrm{d}} = \arg\min_{r_{\mathrm{d}}} \varepsilon\left(r_{\mathrm{d}}\right). \quad (8)$$

The version of the LVC scheme implementing the Optimal Subchannel Provisioning (OSP) with the Impulse noise Correction (IC) is denoted LVC-OSP-IC in what follows.

4. SIMULATION

In this section, four variants of LVC schemes are compared. The first one is a baseline LVC with No Impulse noise Correction (LVC-NIC). The number of transmitted chunks is only constrained by the bandwidth and total power constraints. The second one is a LVC-WSP scheme with No Impulse noise correction (LVC-WSP-NIC), a proportion r_{d} of subchannels is not used for chunk transmission, the remaining chunks benefit from more transmission power. In LVC-NIC and LVC-WSP-NIC, the effect of the impulse noise is taken into account by an increase of the variance of the background noise from σ_i^2 to $p_{\mathrm{I}}\sigma_{\mathrm{I}}^2 + \sigma_i^2$ in the precoding and decoding matrix design [11,29]. The third one is the LVC-WSP-IC of Section 2. The last one is the LVC-OSP-IC of Section 3.3. The situations in absence of impulse noise denoted as LVC Without Impulse noise (LVC-WoI) and LVC-WSP Without Impulse noise (LVC-WSP-WoI) are considered respectively as references. The simulation parameters are detailed in Section 4.1. Simulation results are described in Section 4.2. The variances of chunks and channel characteristics are transmitted as metadata as in SoftCast [9]. The resulting rate is neglected in here.

4.1. Simulation parameters

Two video sequences are taken from the MPEG test set used for the standardization of HEVC [17], namely BQSquare (Class D) and RaceHorses (Class C) with a frame rate 60 and 30 respectively. One considers only the luminance component of each video. Consider OFDM subchannels with a bandwidth $f_{\mathrm{SC}} = 24.414$ kHz. Using analog QAM and root-raised-cosine Nyquist filters with $\beta_{\mathrm{r}} = 30\,\%$ roll-off, one obtains a per-subchannel transmission rate $r_{\mathrm{SC}} = \frac{2f_{\mathrm{SC}}}{1+\beta_{\mathrm{r}}}$. The number n_{SC} of subchannels for transmission are respectively 256 and 416 for BQSquare and RaceHorses. The GoP size n_{F} is 8 frames. The chunk size $n_{\mathrm{r}} \times n_{\mathrm{c}}$ is 30×32. Given these values, we assume there are 768 and 3328 chunks can be transmitted per GoP for BQSquare and RaceHorses respectively. In the FBMP, 5 dominant impulse noise positions vectors are considered for correction, which represents a compromise between complexity and performance as shown in [18]. The power constraint p_{T} for one OFDM symbol is set with 2560. The variance and the probability of impulse noise are $\sigma_{\mathrm{I}}^2 = 100$ and $p_{\mathrm{I}} = 0.01$ or $p_{\mathrm{I}} = 0.02$.

4.2. Simulation results

4.2.1. Impact of r_d on the efficiency of impulse noise mitigation

The average PSNR of the first 5 GoPs of BQSquarre and RaceHorses is evaluated for SNRs ranging from 0 dB to 20 dB. SNR accounts only for the Gaussian noise, while the impulse noise power is considered via the INR. INR is computed from SNR, p_{T}, n_{SC}, and σ_{I}^2. A simulation result is shown in Fig. 2. We can see that when r_{d} increases, the impulse noise correction improves. Fig. 3 represents the gains obtained by LVC-WSP-IC compared to LVC-NIC at different SNRs and for different target values of r_{d} taken in $\mathcal{R} = \{0.25, 0.33, 0.41, 0.5, 0.66, 0.75\}$. One observes that the optimal value of r_{d} depends on the value of the channel SNR. At low SNRs, r_{d} should be large, whereas at large SNRs, r_{d} may be reduced. This is mainly due to the fact that at low SNR, the INR is low and impulse noise identification is difficult with few syndrome samples. At high SNR, the INR increases, and it becomes easier to identify the samples affected by impulse noise.

4.2.2. Optimal subchannel provisioning

The performance of LVC-OSP-IC and LVC-WSP-IC is compared in Fig. 4. LVC-WSP-IC selects the best r_{d} in $\mathcal{R}$ for each value of the SNR. In most of the cases, LVC-OSP-IC which searches for r_{d} in the interval $[0.15, 0.75]$ to evaluate (6), provides better results with a gain in PSNR up to 0.2 dB. In some cases, LVC-OSP-IC is slightly worse than LVC-WSP-IC due to the mismatch of the PM compared to the real performance. Nevertheless, the PNSR loss remains less than 0.05 dB. This confirms the quality

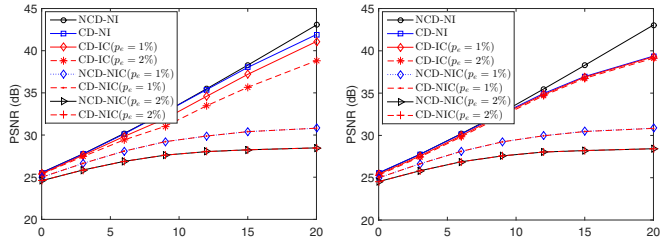

(a) $r_d = 0.25$ (b) $r_d = 0.5$

Fig. 2: PSNR evolution as a function of SNR (dB) and r_d for BQSquare when $\sigma_I^2 = 100$

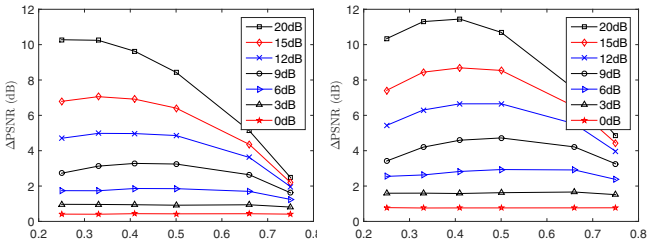

(a) $p_I = 0.01$ (b) $p_I = 0.02$

Fig. 3: PSNR gain of LVC-WSP-IC compared to LVC-NIC for different r_d for BQSquare when $\sigma_I^2 = 100$,

of the PM to predict the impulse noise correction performance of the FBMP algorithm. Finally, Fig. 5 shows the first reconstructed frame of RaceHorses with LVC-NIC and LVC-OSP-IC when $\sigma_I^2 = 100$, $p_I = 0.01$, SNR $= 15$ dB. A gain of 7.8 dB is observed with LVC-OSP-IC. Reconstructed videos, including one additional test sequence (BasketballDrill) are available at *https://drive.google.com/drive/folders/13LB5nR3nY79bF3CEMUl41HY4Bc_ekhBF*.

4.2.3. Analysis of the effect of mismatched channel conditions

In the following experiments, the channel SNR is set equal to 20 dB and $\sigma_I^2 = 100$. One considers several target impulse noise probabilities p_{It} chosen equal to 0%, 0.5%, 1%, or 2% for the LVC-OSP-IC scheme. The PSNR of the decoded video for actual impulse noise probabilities p_I ranging from 0% to 4% are shown in Figure 6. In the simulation, at receiver side, the actual parameter values are used for impulse noise correction (FBMP algorithm) and decoding matrix computation (Section 3.1). As expected, the performance is best when p_I matches p_{It}. Choosing a large p_{It} improves the robustness to a larger p_I, but the price to be paid is a lower PSNR when p_I is smaller than p_{It}. It also shows that even if a small $p_{It} = 0.5\%$ is chosen, in case of mismatch, the PSNR decrease is much smoother than in absence of subchannel provisioning for impulse noise mitigation. This solution can thus be adapted to a multicast scenario.

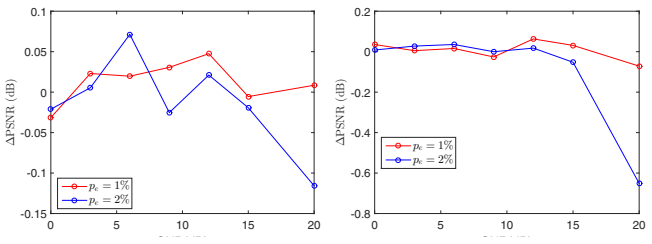

(a) BQSquare (b) RaceHorse

Fig. 4: PSNR differences between LVC-OSP-IC and LVC-WSP-IC

(a) LVC-NIC: PSNR=30.83dB (b) LVC-OSP-IC: PSNR=38, 64dB.

Fig. 5: First frame of RaceHorses. $\sigma_I^2 = 100$, $p_I = 0.01$ and SNR=15dB. (a) by using LVC-NIC; (b) by using LVC-OSP-IC.

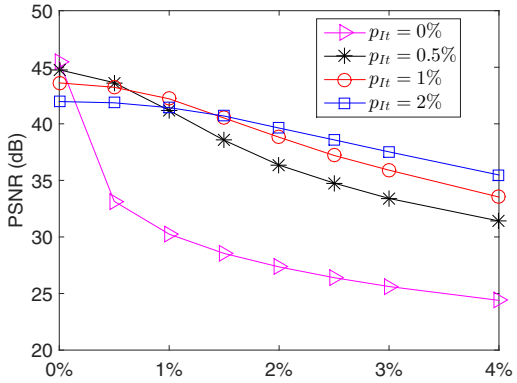

Fig. 6: Effect of the mismatch between p_{It} and p_I when SNR $=$ 20 dB and $\sigma_I^2 = 100$ (for the RaceHorses video sequence)

5. CONCLUSION

This paper considers SoftCast-based video transmission schemes affected by impulse noise. The FBMP algorithm is adapted for impulse noise mitigation. This requires the provisioning of some subchannels on which no information is transmitted. In this case the nominal PSNR decreases in absence of impulse noise. A trade-off has thus to be found between impulse noise correction efficiency and nominal PSNR reduction. To address this problem, a PM model is proposed to evaluate the variance of the impulse noise residual after mitigation. This model allows one to estimate the optimal number of subchannel to provision for impulse noise mitigation. The performance of proposed LVC-OSP-IC scheme has been evaluated on two reference video sequences. The performance is significantly better than a baseline LVC scheme without correction.

Future work will be dedicated to the evaluation of the optimal number of subchannels to provision for impulse noise mitigation in case of LVC under multicast situation.

6. REFERENCES

[1] Tareq Y Al-Naffouri, Ahmed A Quadeer, and Giuseppe Caire. Impulse noise estimation and removal for ofdm systems. *IEEE Transactions on Communications*, 62(3):976–989, 2014.

[2] M. Cagnazzo and M. Kieffer. Shannon-Kotelnikov mappings for SoftCast-based joint source-channel video coding. In *Proc. IEEE ICIP*, pages 1085–1089. IEEE, 2015.

[3] Rafael E Carrillo, Ana B Ramirez, Gonzalo R Arce, Kenneth E Barner, and Brian M Sadler. Robust compressive sensing of sparse signals: a review. *EURASIP Journal on Advances in Signal Processing*, 2016(1):108, 2016.

[4] H. Cui, Z. Song, Z. Yang, C. Luo, R. Xiong, and F. Wu. Cactus: A hybrid digital-analog wireless video communication system. In *Proc. ACM Int. Conf. on Modeling, Analysis & Simulation of Wireless and Mobile Systems*, pages 273–278, 2013.

[5] X. Fan, F. Wu, D. Zhao, and O. C. Au. Distributed wireless visual communication with power distortion optimization. *IEEE Trans. Circuits and Systems for Video Technology*, 23(6):1040–1053, 2013.

[6] X. Fan, R. Xiong, F. Wu, and D. Zhao. Wavecast: Wavelet based wireless video broadcast using lossy transmission. In *Proc. IEEE VCIP*, pages 1–6, San Diego, CA, 2012.

[7] Xiaopeng Fan, Ruiqin Xiong, Debin Zhao, and Feng Wu. Layered soft video broadcast for heterogeneous receivers. *IEEE Trans. Circuits Syst. Video Techn.*, 25(11):1801–1814, 2015.

[8] D. He, C. Lan, C. Luo, E. Chen, F. Wu, and W. Zeng. Progressive pseudo-analog transmission for mobile video streaming. *IEEE Trans. Multimedia*, 19(8):1894–1907, 2017.

[9] S. Jakubczak and D. Katabi. Softcast: Clean-slate scalable wireless video. In *Proc. 48th Annual Allerton Conference on Communication, Control, and Computing*, pages 530–533, 2010.

[10] Cuiling Lan, Chong Luo, Wenjun Zeng, and Feng Wu. A practical hybrid digital-analog scheme for wireless video transmission. *IEEE Transactions on Circuits and Systems for Video Technology*, 28(7):1634–1647, 2018.

[11] K. H. Lee and D. P. Petersen. Optimal linear coding for vector channels. *IEEE Trans. On Communications*, 24(12):1283–1290, 1976.

[12] Jing Lin, Marcel Nassar, and Brian L Evans. Impulsive noise mitigation in powerline communications using sparse bayesian learning. *IEEE Journal on Selected Areas in Communications*, 31(7):1172–1183, 2013.

[13] X. L. Liu, W. Hu, C. Luo, Q. Pu, and F. Wu. Compressive image broadcasting in MIMO systems with receiver antenna heterogeneity. *Signal Processing: Image Communication*, 29(3):361–374, 2014.

[14] X. L. Liu, W. Hu, C. Luo, Q. Pu, F. Wu, and Y. Zhang. Parcast+: Parallel video unicast in MIMO-OFDM WLANs. *IEEE Trans. Multimedia*, 16(7):2038–2051, 2014.

[15] Xiao Lin Liu, Wenjun Hu, Qifan Pu, Feng Wu, and Yongguang Zhang. Parcast: Soft video delivery in mimo-ofdm wlans. In *Proceedings of the 18th annual international conference on Mobile computing and networking*, pages 233–244. ACM, 2012.

[16] N. H. Nedev. *Analysis of the impact of impulse noise in digital subscriber line systems*. PhD thesis, The University of Edinburgh, 2003.

[17] J.-R. Ohm, G. J. Sullivan, H. Schwarz, T. K. Tan, and T. Wiegand. Comparison of the coding efficiency of video coding standards–including high efficiency video coding (HEVC). *IEEE Trans. Circuits and Systems for Video Technology*, 22(12):1669–1684, 2012.

[18] Philip Schniter, Lee C Potter, and Justin Ziniel. Fast bayesian matching pursuit. In *Information Theory and Applications Workshop, 2008*, pages 326–333. IEEE, 2008.

[19] Z. Song, R. Xiong, S. Ma, X. Fan, and W. Gao. Layered image/video SoftCast with hybrid digital-analog transmission for robust wireless visual communication. In *Proc. IEEE ICME*, pages 1–6, 2014.

[20] G. J. Sullivan, J.-R. Ohm, W.-J. Han, and T. Wiegand. Overview of the high efficiency video coding (HEVC) standard. *IEEE Trans. Circuits Syst. Video Technol.*, 22(12):1649–1668, 2012.

[21] T. Wiegand, G. J. Sullivan, G. Bjøntegaard, and A. Luthra. Overview of the H.264/AVC video coding standard. IEEE *Trans. on Circuits and Systems for Video Technology*, 13(7):560–576, 2003.

[22] M. Wien, H. Schwarz, and T. Oelbaum. Performance analysis of SVC. *IEEE Trans. Circuits and Systems for Video Technology*, 17(9):1194–1203, 2007.

[23] R. Xiong, F. Wu, X. Fan, C. Luo, S. Ma, and W. Gao. Power-distortion optimization for wireless image/video SoftCast by transform coefficients energy modeling with adaptive chunk division. In *Proc. IEEE VCIP*, pages 1–6, 2013.

[24] R. Xiong, F. Wu, J. Xu, X. Fan, C. Luo, and W. Gao. Analysis of decorrelation transform gain for uncoded wireless image and video communication. *IEEE Trans. Image Processing*, 25(4):1820–1833, 2016.

[25] R. Xiong, J. Zhang, F. Wu, J. Xu, and W. Gao. Power distortion optimization for uncoded linear transformed transmission of images and videos. *IEEE Trans. Image Processing*, 26(1):222–236, 2017.

[26] L. Yu, H. Li, and W. Li. Wireless scalable video coding using a hybrid digital-analog scheme. *IEEE Trans Circuits and Systems for Video Technology*, 24(2):331–345, 2014.

[27] F. Zhang, A. Wang, H. Wang, S. Li, and X. Ma. Channel-aware video SoftCast scheme. In *Proc. IEEE ChinaSIP*, pages 578–581, Chengdu, China, 2015.

[28] Z. Zhang, D. Liu, X. Ma, and X. Wang. Ecast: An enhanced video transmission design for wireless multicast systems over fading channels. *IEEE Systems Journal*, 11(4):2566–2577, 2017.

[29] S. Zheng, M. Antonini, M. Cagnazzo, L. Guerrieri, M. Kieffer, I. Nemoianu, R. Samy, and B. Zhang. SoftCast with per-carrier power-constrained channels. In *Proc. IEEE ICIP*, pages 2122–2126, 2016.

[30] Manfred Zimmermann and Klaus Dostert. Analysis and modeling of impulsive noise in broad-band powerline communications. *IEEE transactions on Electromagnetic compatibility*, 44(1):249–258, 2002.